Thermochimica Acta, 11 (1975) 409–424

THERMAL STABILITIES OF ISOELECTRONIC, ISOSTRUCTURAL NITRATES, CARBONATES AND BORATES

M. SWEENEY
University of the West Indies (Trinidad)
(Received 23 September 1974)

ABSTRACT

The effects of temperature changes on an iso-electronic, iso-structural group of compounds containing an iso-electronic, iso-structural complex of ions were studied. The stability of the nitrates is discussed on the basis of their temperature of fusion and solid state transitions; the carbonates from their decomposition temperatures and solid state transitions; and the borates on solid state transitions. The order of thermal stabilities is found to be $ABO_3 > A'CO_3 > A''NO_3$.

INTRODUCTION

In this study a group of compounds was chosen with the general formula of AMO_3 under the restriction that the MO_3 group is planar. The group includes the univalent nitrates, the divalent carbonates and the trivalent borates. The univalent nitrates are the group IA or alkali metal nitrates; the divalent carbonates are the group IIA or alkaline earth carbonates; the trivalent borates are the group IIIB metal borates and indium borate is from group IIIA.

The oxidized state of the group IA, IIA and IIIB metals results from the loss of one, two and three electrons, respectively. These cations possess the inert gas structure with filled $(n-1)$ s and $(n-1)$ p orbitals. There are no electrons in the valence shell. The oxidized state of indium is plus three, but the s, p, and d sub-shells are filled.

The compounds were so chosen that each would possess, or upon transformation would gain, the same crystal structure, namely, the calcite structure.

EXPERIMENTAL

General

Thermal experimental methods for characterizing the system by measuring changes in physico-chemical properties at elevated temperatures as a function of linear increases in temperatures were used. The two chief methods are: (a) The DTA in which the changes in 'heat content' are measured as a function of increasing temperature; and (b) the TG in which changes in weight are measured under similar conditions.

These two techniques provide information relating to physical and chemical phenomena such as, for example: crystalline transitions, fusions, vaporizations, decompositions, solid-state reactions and dehydrations.

X-ray diffraction studies and thermal microscopic analyses were used to provide supporting information.

Sample

The nitrates and carbonates investigated, with the exception of magnesium carbonate, were standard industrial compounds. The borates and magnesium carbonate had to be prepared. All materials were ground and sieved to 140–300 mesh size. Runs were done under three sets of conditions, viz., undiluted samples, samples diluted with calcined alumina and samples diluted with calcined magnesia. Calcined alumina was used in the reference cell unless the sample was diluted with calcined magnesia, in which case magnesia was used as the blank also. X-ray patterns were made of the initial samples and final residues from the DTA and TG analyses.

Procedure

The DTA apparatus was calibrated with analar sodium nitrate (for the temperature range 150–500 °C) and calcium carbonate (500–1000 °C). It was regularly recalibrated with calcium carbonate.

In order to calculate the true weight changes from the observed (apparent) weight changes, a thermograph of the empty crucible was obtained prior to its use for sample analyses. This was used as a correction curve on the TG weight changes in the samples.

Film shrinkages in the high temperature X-ray analyses were corrected by the Straumanis[1] technique.

RESULTS AND DISCUSSIONS

General

Data obtained by DTA and TG studies on an iso-electronic, iso-structural series of compounds with the general formula AMO_3 are shown in Tables 1–6 and Figs. 1–8. The several curves obtained under different experimental conditions are presented in a separate figure for each compound. It can be seen that not only do the shapes of the curves and peaks differ somewhat in DTA and TG traces, but also that dilution with alumina and magnesia affects the results to a greater or lesser degree.

The peak temperatures, heats of reaction, and change of mass are given in summary in the tables. The temperatures at the peak of the DTA curves are shown in Table 1, and at the peaks of the weight-loss curves in Table 2. The energy of reaction, weight-loss data and summary of decomposition on some nitrates are given in Tables 4A, B, and C, respectively. Table 5 shows the DTA results for the initial mixtures used in preparing the borates.

The carbonates

Among the carbonates, magnesite and calcite each gave a single maximum in both DTA and TG (Figs. 1 and 2). Strontianite and witherite were not so simple, showing more peaks in DTA than in TG, and giving curves with more complex shapes than the decomposition curve for calcite in all cases.

A comparison of the DTA and TG curves for strontianite (Fig. 3) indicates that the first reaction is a transition at 925±3°C. This is from the aragonite to the calcite structure[2]. This solid–solid transition is also present in the mixtures. The diluted samples, however, exhibited a more complex decomposition pattern than the undiluted strontianite. In the TG pattern of the strontianite–alumina mixture there are shoulders at 720 and 880°C (Table 3B and Fig. 3). There are no corresponding DTA peaks for these shoulders, showing their small energy component compared to the solid-state transition at 925°C. In the TG thermogram of the strontianite–magnesia mixture there is a shoulder at 975–1020°C preceding the main peak at 1075°C. This shoulder apparently correlates with the DTA peak at 1072°C and can presumably be associated with a solid-state reaction between sample and diluent. Whether this diluent is alumina or magnesia, the final step in the decomposition is affected, the reaction temperature being somewhat lower in both DTA and TG.

TABLE 1

DTA PEAK TEMPERATURES

Sample	*Temperature at peak of thermograph*	
	Transition	*Decomposition*
$MgCO_3$		450
$MgCO_3$–Al_2O_3		400
$MgCO_3$–MgO		400
$CaCO_3$		900
$CaCO_3$–Al_2O_3		850
$CaCO_3$–MgO		850
$SrCO_3$	925	1150
$SrCO_3$–Al_2O_3	922	1102
$SrCO_3$–MgO	928	1072, 1145
$BaCO_3$	815, 983	1233
$BaCO_3$–Al_2O_3	800, 970	1190
$BaCO_3$–MgO	808, 970	1220
$LiNO_3$–Al_2O_3	257, 340[a]	615, 678, 700, 776, 960[a]
$LiNO_3$–MgO	266, 327[a]	707, 749, 771, 1002, 1084
$NaNO_3$–Al_2O_3	272[a], 316	733, 904
$NaNO_3$–MgO	293[a], 337	756, 893, 1020
KNO_3–Al_2O_3	137, 337	685, 814, 924
KNO_3–MgO	165, 369	754, 980, 1080
$CsNO_3$–Al_2O_3	150, 410	920
$CsNO_3$–MgO	160, 418	943
YBO_3	1021	
$ScBO_3$, $LaBO_3$, $InBO_3$	No peaks	

[a] Shoulders only, ΔH values unobtainable.

Witherite, like strontianite and unlike calcite, does not decompose from its low temperature structure, but passes through two solid transitions prior to decomposition[2]. The three DTA peaks of witherite (Fig. 4) represent transitions from the alpha to the beta form at 808±8°C, from the beta to the gamma form at 976±7°C and finally the decomposition of the gamma form to barium oxide and carbon dioxide.

The TG data (Table 3) in the undiluted carbonates showed a stoichiometric loss of carbon dioxide. In the cases of $MgCO_3$, $SrCO_3$ and $BaCO_3$ mixtures with MgO, the loss was greater than expected. This loss is presumably due to moisture in the diluent. The $BaCO_3$–Al_2O_3 mixture gave a loss of carbon dioxide which was less than expected. This may be due to the solid-state reaction between this material and the diluent. It may also be noticed that the TG curves were less complex for diluted than for undiluted witherite (Fig. 4). The TG data indicated recarbonation in all cases with the undiluted carbonates and in some cases with the diluted samples (Table 3).

The results from DTA (Table 1) and TG (Table 2) show the relative thermal stabilities of the carbonates which decrease in the order $BaCO_3 > SrCO_3 > CaCO_3 >$

TABLE 2
PEAK TEMPERATURES AT THE WEIGHT-LOSS CURVES

Sample	*Temperature at peak of thermographs*
$MgCO_3$	420
$MgCO_3$–Al_2O_3	370
$MgCO_3$–MgO	370
$CaCO_3$	870
$CaCO_3$–Al_2O_3	820
$CaCO_3$–MgO	820
$SrCO_3$	1100
$SrCO_3$–Al_2O_3	720, 880[a], 1020
$SrCO_3$–MgO	1075
$BaCO_3$	1225, 1310
$BaCO_3$–Al_2O_3	1185
$BaCO_3$–MgO	1185
$LiNO_3$	700
$LiNO_3$–Al_2O_3	615
$LiNO_3$–MgO	725
$NaNO_3$	798
$NaNO_3$–Al_2O_3	670, 740, 870, 1030
$NaNO_3$–MgO	690, 880, 1050[a]
KNO_3	790, 1060
KNO_3–Al_2O_3	810, 950
KNO_3–MgO	780, 885, 970, 1130
$CsNO_3$–Al_2O_3	280, 640, 910
$CsNO_3$–MgO	905
ABO_3's	No peaks

[a] Shoulders.

$MgCO_3$. The energy of decomposition for $BaCO_3$ (Table 3A) should not be given too much significance, since the reaction between BaO and the thermocouples[3] will create a simultaneous exothermic effect which will cancel out some of the endothermic effect caused by the decomposition reaction. The result of these opposing factors will be a decrease in area of the reaction curve, and consequently, a decrease in the calculated energy involved. Since the extent of this reaction is dependent on the amount of BaO in contact with the thermocouple at any particular time, and this amount is not known, the overall result is insignificant. It is interesting to note, however, that unlike all the other substances studied, the decomposition energy of a mixture—with alumina in this particular case— is higher than that of the undiluted samples. The transition energies of witherite are certainly significant since they correspond with the solid-state transitions of $BaCO_3$. The total energy of transitions of $BaCO_3$ is greater than the transition in $SrCO_3$ (Table 4).

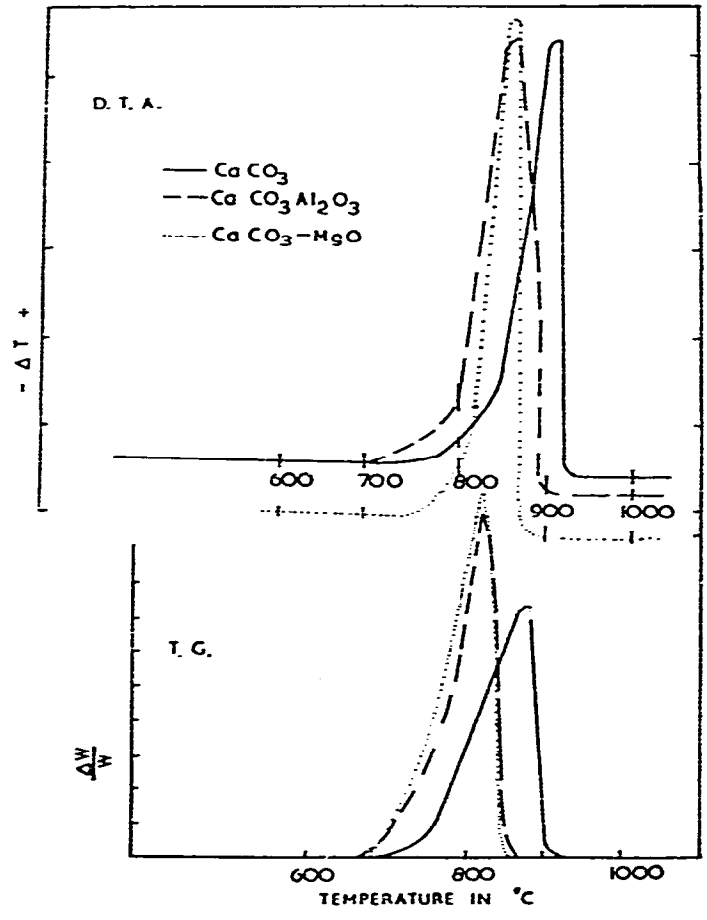

Fig. 1. DTA and TG curves for $CaCO_3$ and diluents.

The nitrates

Unlike the carbonates which decomposed from the solid state, the nitrates melted first. They then decomposed from the molten state in a complex way over a substantial temperature range. There was, however, a transition to the calcite structure before fusion. As usual, the DTA peaks were absent in the TG thermographs, corresponding to transitions and phase changes (Figs. 5 and 8). The temperature range that showed activities in both techniques corresponded with the decomposition reactions. From the multiplicity of maxima, and the close overlapping of adjacent curves in both DTA and TG the decompositions clearly consist of a complex number of successive reactions. The addition of a diluent can influence the decomposition, and may affect one part of the complex reaction more than another.

The first DTA peak of lithium nitrate (Fig. 5) is due to fusion and the second (rounded) is not yet understood. The first and very small endotherm of sodium nitrate (Fig. 6) is due to a second order transition and the second larger peak is due to fusion. The first peak of potassium nitrate (Fig. 7) is a solid–solid transition from the aragonite to calcite structure and the second is due to fusion.

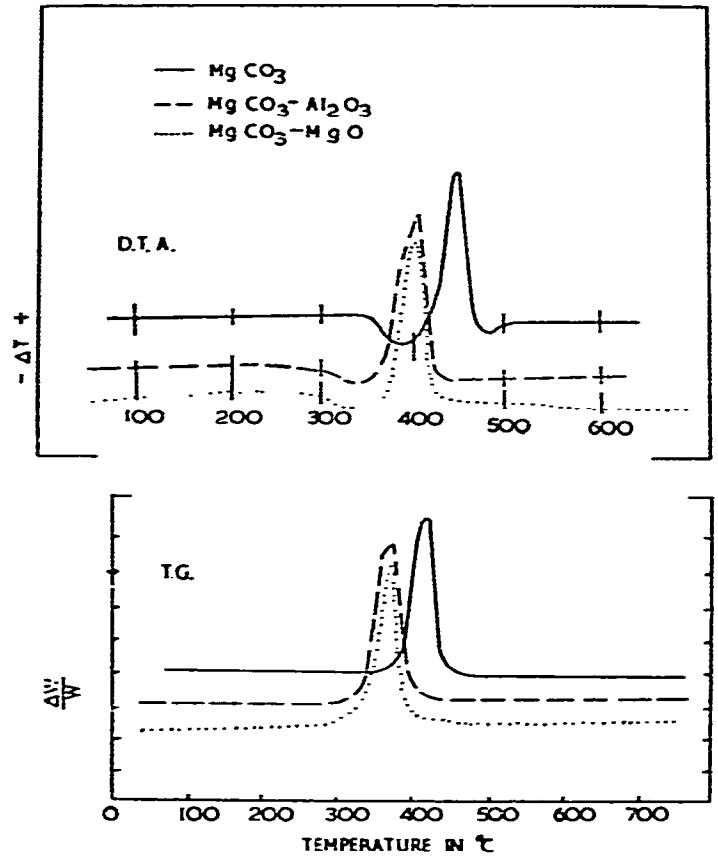

Fig. 2. DTA and TG curves for $MgCO_3$ and diluents.

TABLE 3A

ENERGY OF REACTION OF SOME CARBONATES[a]

Sample	*Transition*		*Decomposition*	
	Lit.	*Exp.*	*Calc.*	*Exp.*
$MgCO_3$			121.3	121.3
$MgCO_3$–Al_2O_3				120.5
$MgCO_3$–MgO				122.6
$CaCO_3$			201.7	201.7
$CaCO_3$–Al_2O_3				201.7
$CaCO_3$–MgO				201.7
$SrCO_3$	16.65	15.10	258.6	231.8
$SrCO_3$–Al_2O_3		14.27		131.0
$SrCO_3$–MgO		14.73		222.2
$BaCO_3$	14.85; 2.89	16.57; 2.26	291.2	79.08
$BaCO_3$–Al_2O_3		13.64; 2.18		101.7
$BaCO_3$–MgO		15.48; 2.26		74.89

[a] The heats of reaction were calculated from the heats of formation. (The experimental heats of decomposition of barium carbonate and mixtures are not significant since barium oxide reacts with the platinum of the Pt/Pt–10% Rh thermocouples.)

$$\Delta H_r = \Delta H_f + \int_{T_2}^{T_1} \Delta C_p \mathrm{d}T.$$

TABLE 3B

WEIGHT LOSS DATA OF SOME CARBONATES

Sample	*Wt. of active material*	*Wt. loss*		*% Wt. gained on cooling*
		Calc.[a]	*Exp.*	
$MgCO_3$	0.05300	0.02765	0.02770	3.1
$MgCO_3$–MgO	0.05690	0.02970	0.03440	0.53
$CaCO_3$	0.10265	0.04506	0.04505	18.5
$CaCO_3$–Al_2O_3	0.02976	0.01307	0.01310	2.0
$CaCO_3$–MgO	0.03018	0.01328	0.01330	
$SrCO_3$	0.32940	0.09820	0.09820	9.5
$SrCO_3$–Al_2O_3	0.08000	0.02388	0.02390	5.4
$SrCO_3$–MgO	0.03734	0.01113	0.01170	11.6
$BaCO_3$	0.18810	0.04193	0.04192	4.1
$BaCO_3$–Al_2O_3	0.07714	0.01719	0.01690	1.0
$BaCO_3$–MgO	0.04543	0.01012	0.01020	

[a] Weight loss was calculated on the basis of total loss of carbon dioxide: $ACO_3 \rightarrow AO + CO_2$.

TABLE 4A

ENERGY OF REACTION OF SOME NITRATES[a]

Samples	*Fusion*		*Transition*		*Decomposition*[b]	
	Lit.	*Exp.*	*Lit.*	*Exp.*	*Calc.*	*Exp.*
$LiNO_3$	25.44	—	—	—	78.24	—
$LiNO_3$–Al_2O_3	—	22.64	—	—	—	264.9
$LiNO_3$–MgO	—	22.84	—	—	—	123.0; 130.1
$NaNO_3$	15.90	—	—	—	64.85	—
$NaNO_3$–Al_2O_3	—	16.65	—	—	—	146.9
$NaNO_3$–MgO	—	16.65	—	—	—	243.5
KNO_3	11.72	—	5.44	—	122.6	—
KNO_3–Al_2O_3	—	12.47	—	5.56	—	50.67; 37.24
KNO_3–MgO	—	12.84	—	5.48	—	30.12; 54.81; 80.75
$CsNO_3$	13.60	—	—	—	—	—
$CsNO_3$–Al_2O_3	—	13.97	—	4.44	—	109.6
$CsNO_3$–MgO	—	13.26	—	4.98	—	121.3

[a] The energy of reaction is given in kJ mol^{-1}. The literature values for the heats of fusion and transition were obtained from the National Bureau of Standards Circular 500. The areas of all thermographs which return to the baseline were calculated. Only one area was calculated for multi-peaked thermograph. [b] The heats of decomposition were calculated from the heats of formation given in the NBS circular 500 for the reaction: $ANO_3 \rightarrow ANO_2 + \frac{1}{2}O_2$. The experimental heats of decomposition include both the total decomposition $ANO_3 \rightarrow A_2O + O_2 + N_2$ + mixed oxides, as well as partial volatilization of A_2O. These reaction curves overlap and cannot readily be separated.

TABLE 4B

WEIGHT LOSS DATA OF SOME NITRATES

Samples	*Weight of active material*	*Wt. loss*		*% Loss of oxides*
		Calc.[a]	*Exp.*	
$LiNO_3$	0.26370	0.2068	0.2568	87.9
$LiNO_3$–Al_2O_3	0.13440	0.1052	0.1249	67.5
$LiNO_3$–MgO	0.04846	0.0379	0.0450	67.2
$NaNO_3$	0.05500	0.0201	0.0478	79.4
$NaNO_3$–Al_2O_3	0.05698	0.0206	0.04885	77.6
$NaNO_3$–MgO	0.05597	0.0204	0.04515	68.7
KNO_3	0.09635	0.0511	0.09450	95.9
KNO_3–Al_2O_3	0.05703	0.03025	0.03425	15.0
KNO_3–MgO	0.05052	0.0270	0.04940	95.2
$CsNO_3$	0.09690	0.0309	0.0969	100
$CsNO_3$–Al_2O_3	0.04735	0.0151	0.0231	24.8
$CsNO_3$–MgO	0.09690	0.0309	0.0949	97.0

[a] Weight loss was calculated on the basis of Li_2O, Na_2O, K_2O, and Cs_2O remaining as the non-volatilized decomposition products. The percent loss of oxides indicates how much of these oxides volatilized.

TABLE 4C

DATA SUMMARIZED FROM TABLES 4A AND 4B

Sample	$\Delta H_{calc.}$[a]	L_s[b]	*Vol. %*[c]	$\Sigma\Delta H$[d]	$\Delta H_{exp.}$
$LiNO_3$	209.6	155.2	—	—	—
$LiNO_3$–Al_2O_3	209.6	155.2	282.4	314.2	264.9
$LiNO_3$–MgO	209.6	155.2	283.3	314.6	253.1
$NaNO_3$	277.4	108.8	—	—	—
$NaNO_3$–Al_2O_3	277.4	108.8	328.9	370.3	146.9
$NaNO_3$–MgO	277.4	108.8	287.4	352.3	243.5
KNO_3	322.6	89.96	—	—	—
KNO_3–Al_2O_3	322.6	89.96	62.76	336.0	87.86
KNO_3–MgO	322.6	89.96	398.3	407.1	165.7
$CsNO_3$	361.5	77.40	—	—	—
$CsNO_3$–Al_2O_3	361.5	77.40	103.8	380.7	109.6
$CsNO_3$–MgO	361.5	77.40	405.8	436.4	121.3

[a] $\Delta H_{calc.}$. The heats of decomposition were calculated from the heats of formation of the reactive materials and their decomposition products. These calculations do not include the energies of volatilization or solid-state reactions between reaction products and diluents. The calculations were based on the following reaction only: $ANO_3 \rightarrow \frac{1}{4}A_2O_2 + \frac{1}{4}A_2O + \frac{1}{2}N_2 + \frac{9}{8}O_2$. [b] L_s. The heats of sublimation were obtained from the literature (8). Since TG data (Table 4B) showed evidence of volatilization, this energy was considered in the overall energy of reaction obtained in the DTA results. [c] The percent volatilization was obtained from Table 4B. [d] $\Sigma\Delta H = \Delta H_{calc.} + L_s \times$ vol. %. This value now includes the energy loss as a result of a solid-state reaction between the oxides and diluents. The difference in energy between $\Sigma\Delta H$ and $\Delta H_{exp.}$ is indicative of such a reaction.

TABLE 5

DTA PEAK TEMPERATURES OBTAINED FOR INITIAL MIXTURES USED IN BORATE FORMATIONS (1) AND RESIDUES REANALYSED (2)

	Sample	*Endotherm*	*Exotherm*
(1)	$Sc_2O_3 + H_3BO_3$	173, 185	736
(2)			
(1)	$Y_2O_3 + H_3BO_3$	173, 185	620
(2)		1021	
(1)	$La_2O_3 + H_3BO_3$	173, 430	630, 715, 760
(2)			
(1)	$In(OH)_3 + H_3BO_3$	173, 185, 326, 370, 600	
(2)			

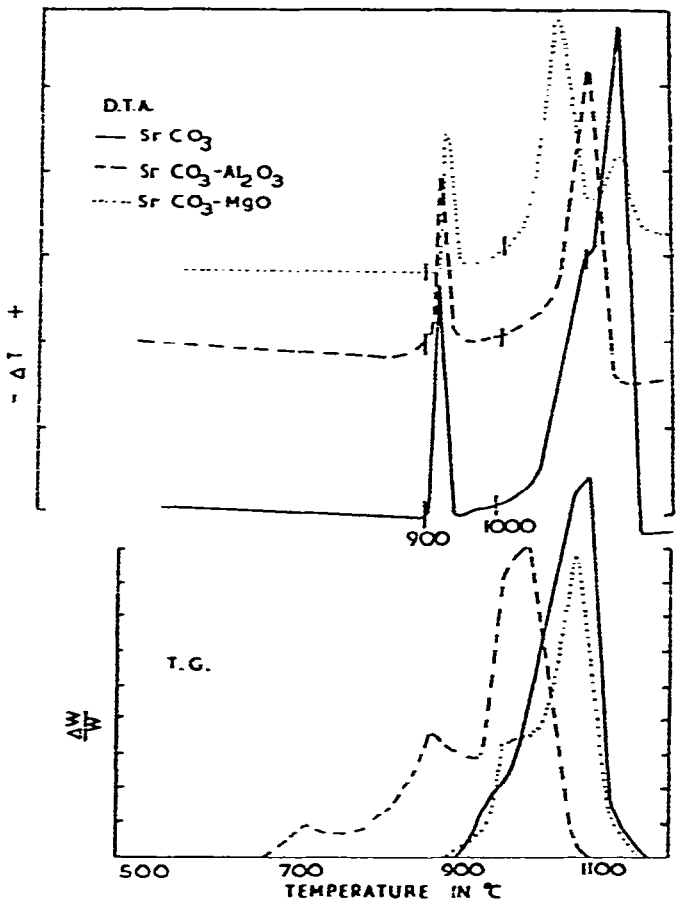

Fig. 3. DTA and TG curves for $SrCO_3$ and diluents.

As in the case of potassium nitrate, the first DTA peak of cesium nitrate (Fig. 8) is a solid-state transition from the aragonite to calcite structure and the second is due to fusion. Unlike the other nitrates, the decomposition thermograph of $CsNO_3$ is relatively simple showing only one decomposition peak.

The TG data (Table 4B) showed that the loss of weight found experimentally was much greater than expected for all the nitrates. The loss indicates that the reaction equation used in calculating the energy changes for the nitrates is not correct. Not only is there no metallic oxide left, but some of the metals are also lost. The percent lost decreases in the order $LiNO_3 > NaNO_3 > KNO_3 > CsNO_3$. As is expected the percent loss is greater for undiluted than for diluted samples.

The thermal stabilities of the nitrates (Table 2) decrease in the order $CsNO_3 > KNO_3 > NaNO_3 > LiNO_3$. The nitrates had to be mixed with the 'so-called' inert materials before a DTA run could be made, since the sample is lost when it melts unless it is absorbed by the solid diluent. However, the heats of decomposition as calculated from NBS data (Table 4) showed that these energies decrease in the order

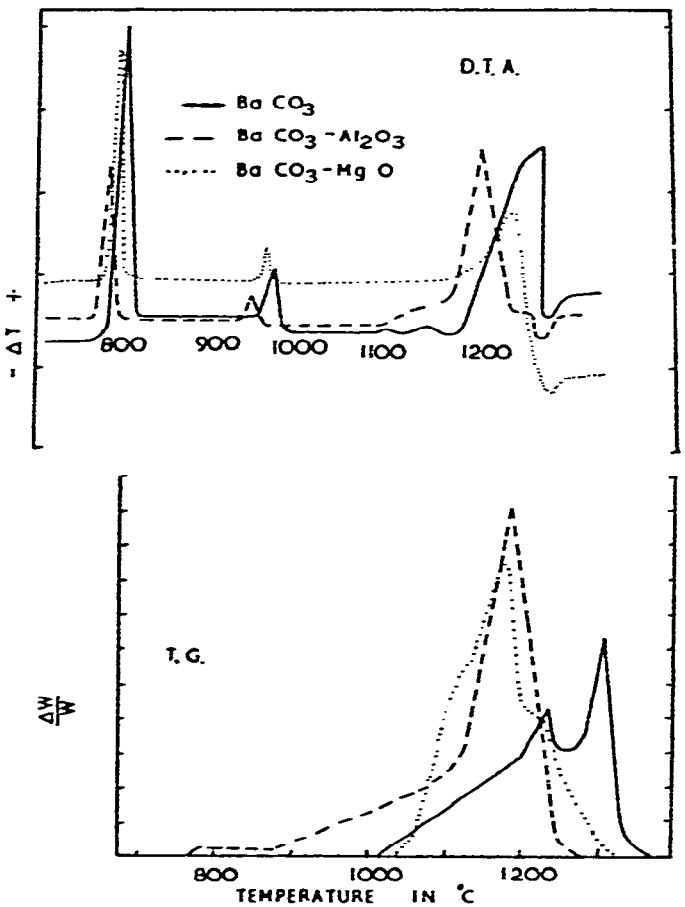

Fig. 4. DTA and TG curves for $BaCO_3$ and diluents.

$CsNO_3 > KNO_3 > NaNO_3 > LiNO_3$. The heats of fusion decreased in the order $LiNO_3 > NaNO_3 > CsNO_3 > KNO_3$.

The borates

In contradistinction to the thermal stabilities of the carbonates and the nitrates, those of the borates are very high, and no decompositions nor fusions occurred within the temperature range of this investigation (Table 5). The TG showed no gain nor loss of weight for any of the borates, and the DTA gave no reaction peak for any of the borates except YBO_3 (Fig. 9). For this substance an endothermic reaction peak was obtained at 1020°C in the heating curve and an exothermic reaction peak in the cooling curve at 580°C. These peaks are due to changes in energy accompanying a solid-state transition. The amount of energy involved was found to be approximately 21 kJ mol^{-1}.

Comparison

Previous investigations have established certain similarities between these iso-electronic, iso-structural compounds. Depending on the value of the radius ratio of the metallic cation to the complex ion, the low temperature structure is isomorphous with either the calcite or the aragonite forms of calcium carbonate[5]. The thermal stability within a given series is known to increase with increasing weight of the metallic cation[6]. It is shown[7] that the phase transition in the alkali metal nitrates and alkaline earth carbonates have a number of features in common. The borates are expected to undergo transitions similar to those observed in the nitrates and carbonates, since the NO_3^-, CO_3^{2-}, and BO_3^{3-} ions are almost morphologically identical. All but one of the borates exist as the calcite structure at room temperature; $LaBO_3$ exists in the aragonite form. Experimental evidence indicated a high temperature transition in YBO_3, which is apparently identical to that from the calcite to the vaterite structure in $CaCO_3$. It follows therefore, that at a sufficiently high temperature $LaBO_3$ would undergo a transformation to the calcite structure. As a result of the stronger electrostatic and repulsive forces acting between the triply charged ions of the A^{3+} and BO_3^{3-} ion in the ABO_3 crystal lattice as compared with the forces between the doubly charged ($A'CO_3$) ions, the transition temperature (arag → calcite) is expected to be higher for the ABO_3 compounds. The order of the thermal stabilities of the different compounds is $ABO_3 > A'CO_3 > A''NO_3$.

The borates did not decompose within the temperature range used in this study. The carbonates decomposed from the solid state at elevated temperatures, while the

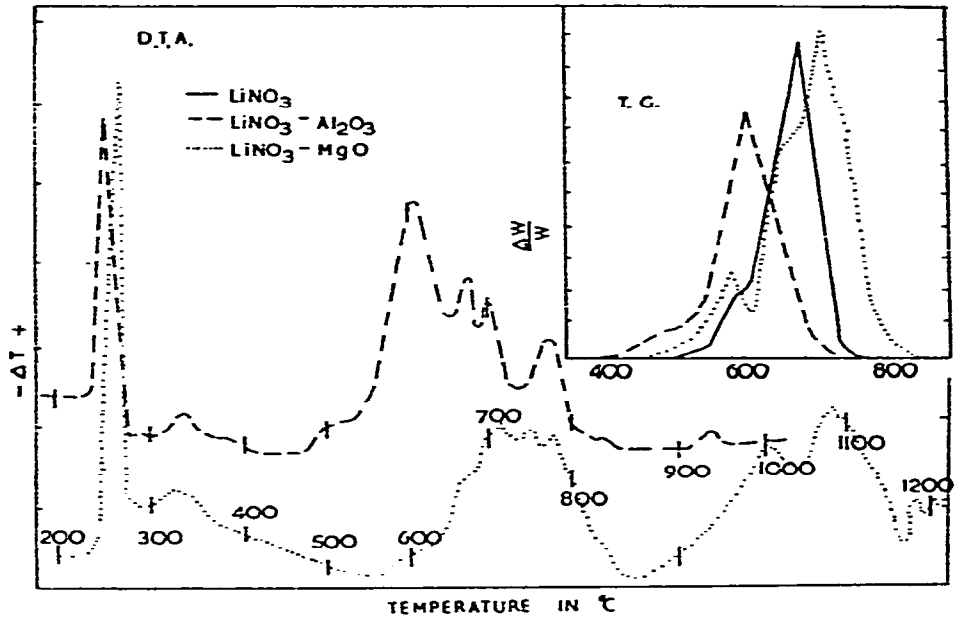

Fig. 5. DTA and TG curves for $LiNO_3$ and diluents.

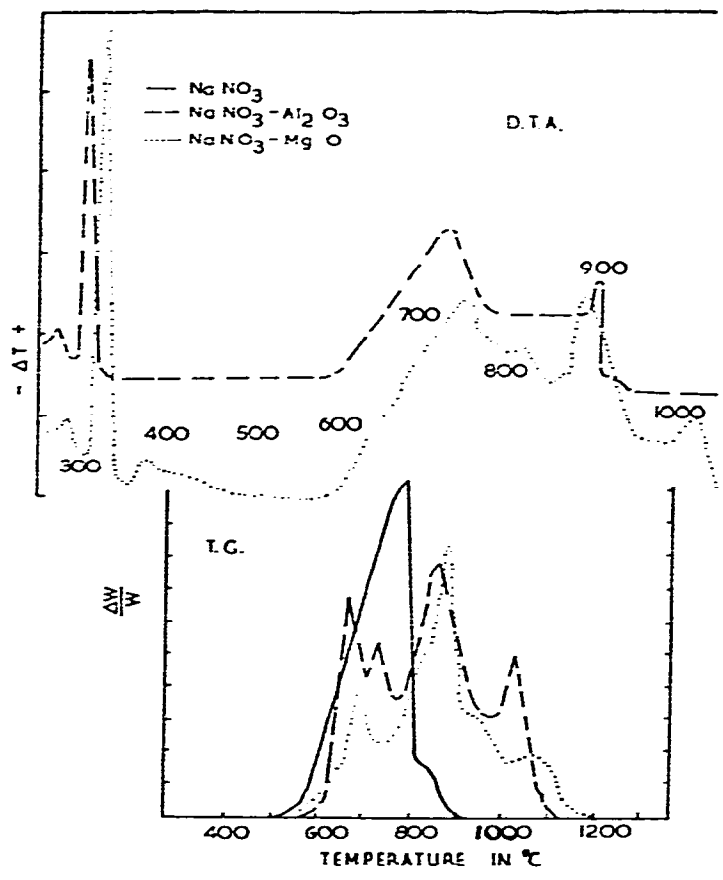

Fig. 6. DTA and TG curves for $NaNO_3$ and diluents.

nitrates first melted at comparatively low temperatures before decomposition started. All decompositions are from the calcite structure.

In compounds that contain a complex ion, the stability of the complex ion becomes a factor which contributes to the thermal stability of the solid as a whole. The lattice energy is a product of the forces between the ions in the solid. Phenomena like fusions and solid-state transitions are reflections of these forces. The melting of the nitrates, aragonite → calcite → vaterite transitions in the carbonates, and the absence of fusions, and for the most part transitions, in the borates, are to be explained in terms related to the energies of the lattice.

In addition, within the lattice the complex ion may decompose. This is a chemical reaction which, of course, also affects the lattice energy since new solids are produced at the same time.

Since fusions and solid-state transitions reflect the lattice energy rather than the stability within the complex anion, the temperatures at which decompositions begin and those at the peak of the decomposition curves form the basis for comparison of the stabilities of these anions. The nitrates were studied only as mixtures on the DTA

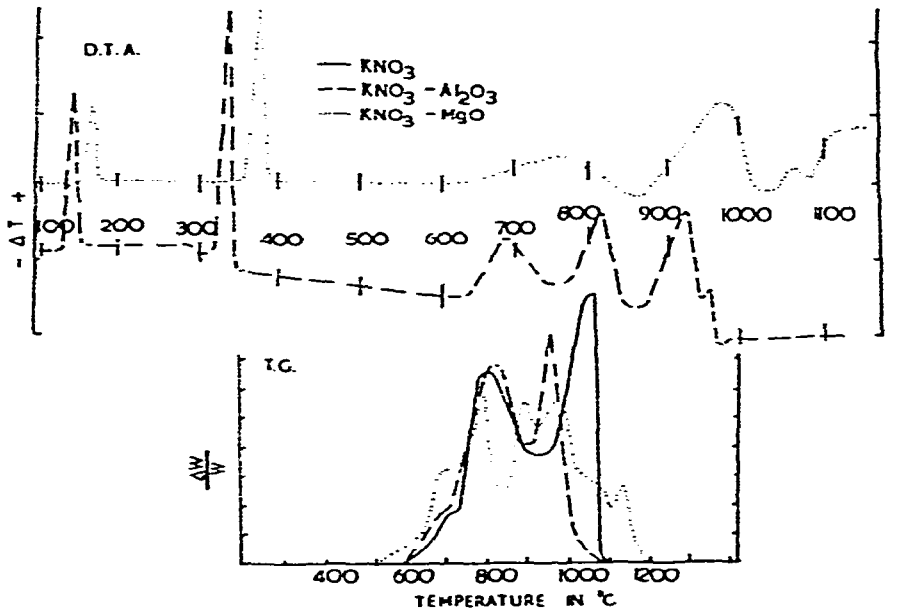

Fig. 7. DTA and TG curves for KNO_3 and diluents.

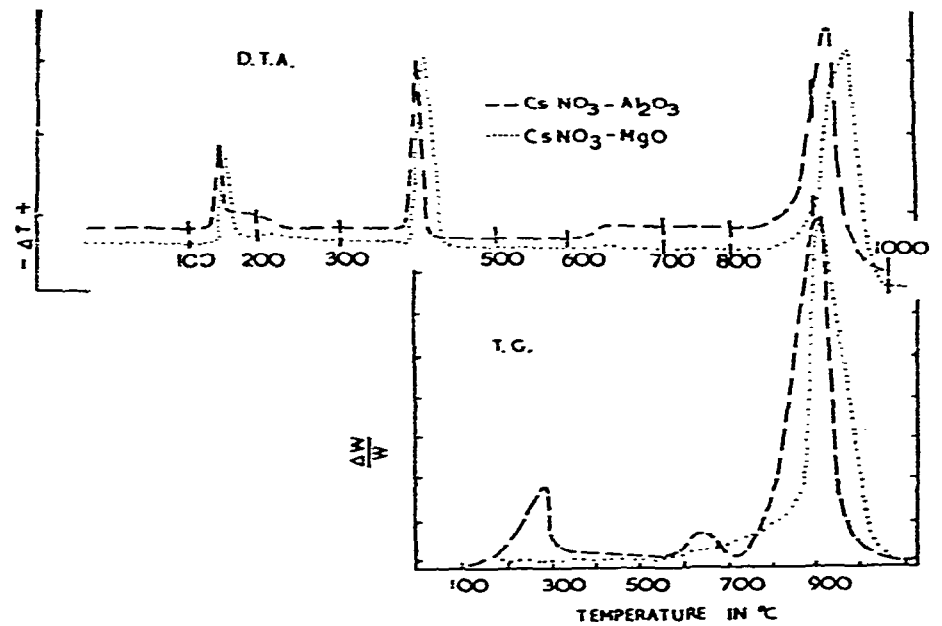

Fig. 8. DTA and TG curves for $CsNO_3$ and diluents.

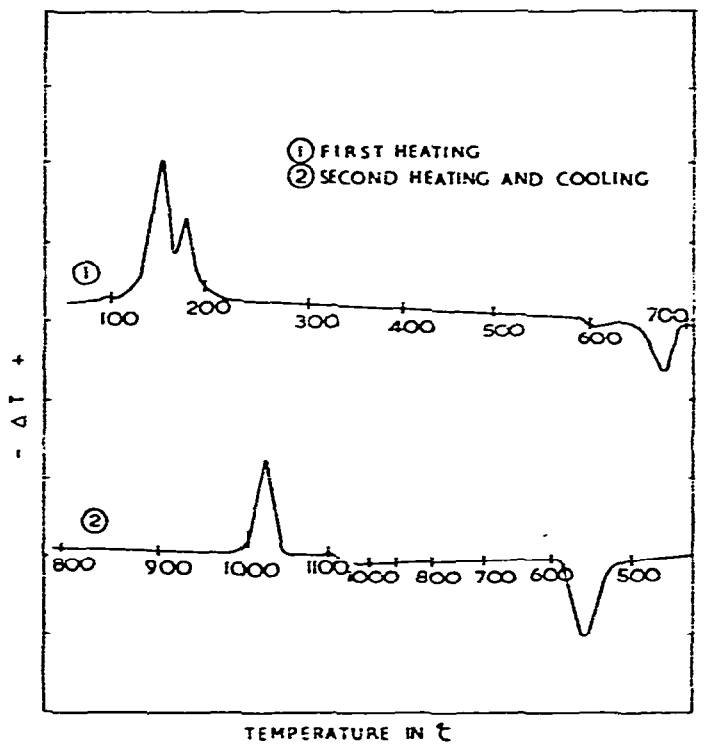

Fig. 9. DTA curves for $Y_2O_3+H_3BO_3$ and YBO_3.

TABLE 6

TEMPERATURE OF DECOMPOSITION

These results are recorded in the absence of diluents on the thermal balance.

Sample	*Decomp. begins*	*Peak temp.*
$LiNO_3$	480	700
$NaNO_3$	520	798
KNO_3	600	790
$CsNO_3$	620	840
$MgCO_3$	380	420
$CaCO_3$	650	870
$SrCO_3$	900	1100
$BaCO_3$	1100	1250
$ScBO_3$	>1350	>1350
YBO_3	>1350	>1350
$LaBO_3$	>1350	>1350
$InBO_3$	>1350	>1350

apparatus and therefore, the TG results of the samples analyzed in the absence of solid diluents were more suitable to compare the thermal stabilities of these materials. The decomposition data were sorted out and are shown in Table 6.

It is evident that the stabilities of the complex ions vary. The differences in the behaviour of these iso-electronic, iso-structural complex ions must, at least in part, be related to the core of the central atoms of these complex ions.

ACKNOWLEDGMENTS

The author wishes to express his thanks and appreciation to Professor W. R. Trost for his advice and constructive criticism on the preparation of this work, and for his suggestions on the project as a whole.

He also wishes to acknowledge the financial aid obtained from the Defence Research Board of Canada, the Canadian Industries Ltd. and Dalhousie University.

REFERENCES

1 *Introductions for Operation of Film Illuminator and Measuring Device, Type 52022/1*, Philips Electronic Instr., Mt. Vernon, New York.
2 H. J. Barchad, *J. Chem. Educ.*, 33 (1956) 103.
3 R. M. Cruver, *J. Amer. Ceram. Soc.*, 33 (1950) 96.
4 H. J. Borchardt and F. Daniels, *J. Phys. Chem.*, 61 (1957) 917.
5 V. M. Goldschmidt and H. Hauptmann, *Nahr. Math. Phys.*, 53 (1932).
6 S. D. Shargorodskii and O. I. Shor, *Ukrain. Khim. Zhur.*, 20 (1954) 357; *Chem. Abstr.*, 49 (1955) 12932.
7 J. J. Lander, *J. Chem. Phys.*, 17 (1949) 892.
8 O. Kubaschewski and E. L. Evans. *Metallurgical Thermochemistry*, Pergamon Press, New York, 1958, Table B.